This is the Pre-Published Version.

The following publication P. Yang, C. K. Tse, J. Xu and G. Zhou, "Synthesis and Analysis of Double-Input Single-Output DC/DC Converters," in IEEE Transactions on Industrial Electronics, vol. 62, no. 10, pp. 6284-6295, Oct. 2015 is available at https://doi.org/10.1109/TIE.2015.2424396.

Synthesis and Analysis of Double-Input Single-Output DC/DC Converter

Ping Yang, Chi K. Tse, *Fellow, IEEE*, Jianping Xu, *Member, IEEE*
and Guohua Zhou, *Senior Member, IEEE*

***Abstract*—This paper describes a systematic procedure using power flow graphs for generating all possible double-input single-output (DISO) DC/DC converters. To maximize the generality of applications, the input ports can possibly be connected with voltage source(s) or current source(s), and the output port can be connected with a voltage load or current load. The control methods are described in this paper. A double-input single-output converter with two voltage sources and one voltage load is taken as an example to analyze a few key properties of practical relevance, including input voltage range, efficiency, power distribution, and switching stress. A popular application of DISO converters involves the use of a battery as storage element, and for this specific case, possible choices for the converters, control method and the attainable efficiency are discussed. Finally, experimental results are presented to verify the analytical results.**

***Index Terms*—Double-input single-output (DISO) converters, Power flow graph, Efficiency analysis, Switching stress, Power distribution**

I. Introduction

MOTIVATED by the increasing use of alternative energy sources, e.g., wind energy, solar energy, fuel cells, etc., multiple-input single-output (MISO) converters have gained popularity in power electronics applications as they are able to capture power from mutually complementary sources and deliver the power to the load [1]-[7]. The conventional approach to converting power from multiple sources is to connect two or more dc voltage sources to independent dc-dc power converters to produce a stable output voltage for the load with an appropriate control arrangement [8]-[10]. Multiple-input converters have been proposed to provide well-regulated output voltage from several input voltage sources connected in parallel [11]-[14]. The simplest form of such converters is the double-input single-output converter (DISO). Pulsating voltage sources along with parallel-connected diodes and pulsating current sources along with series-connected diodes are employed to achieve double-input converters [15], where the input sources are also connected in parallel. In general, for DISO converters, the two input ports can be connected to voltage source(s) or current source(s), and the output port can be connected to a voltage load or current load. Moreover, it is possible that two independent input sources can be connected in series or parallel. Consequently, a number of possible DISO converters should be available to cater for various types of input sources and load terminations. For a double-input converter, the input sources transfer the power to the load through basic switching converters having different efficiencies. The overall efficiency of a DISO converter can thus be optimized by controlling the power flow distribution. Up till now, there has not been systematic synthesis and analysis methods reported for DISO converters that permit convenient and informed choice of circuit configurations and parameters for any given specific application. Furthermore, input ports are normally defined as unidirectional entry ports where power flows into the DISO. However, if one of the input ports is connected to a battery allowing bidirectional power flow, e.g., in a fuel-cell hybrid power system [16], hybrid wind-solar power generation system [17], photovoltaic hybrid generation system [18], etc., the possible choices of converters and control methods will have significant effects on performance and efficiency of the DISO converter.

The objective of this paper is to propose a systematic method to synthesize all possible DISO converters. The control methods of DISO converters with any given type of input sources and loads are discussed. The performance of various DISO converters are compared in terms of the overall efficiency, power flow distribution and switching stress, the aim being to shed light on the characteristics of various configurations thereby providing essential information for designing and constructing DISO converters. A popular example of the DISO converter involves the use of a battery as storage element, and for this case, possible choices for converters, control method and efficiency analysis will be discussed in detail. Finally, experimental results are presented to verify the analytical results.

II. Power Flow Graphs

Power flow graphs were introduced in 2001 for the synthesis of power-factor-correction converters [19], [20]. The concept of power flow is fundamental in power conversion. Despite being a powerful and versatile tool that can yield fruitful and highly effective methods for synthesis and analysis of power converters, *power flow graphs* are still rarely used by researchers and practitioners. In this paper, we deal with the transfer of power from two input ports to an output port

separately or simultaneously, the use of power flow graphs proves to be useful and convenient in describing the way in which power is being transferred among the three ports.For the case of DISO converters with two unidirectional input ports, it should be clear that only two types of power flow sub-graphs, as shown in Fig. 1, are relevant, i.e.,

Type I: Power is transferred from one port to another port, as shown in Fig.1(a).

Type II: Power is transferred from two ports to one port, as shown in Fig.1(b).

Fig. 1. Power flow sub-graphs of DISO converters with both input ports supplying power unidirectionally. (a) Type I; (b) Type II.

Here, the branches in a power flow graph denote the paths of power transmission, and the arrows on the branches indicate the direction of power flow. Based on the power flow sub-graphs shown in Fig. 1, we can construct the complete power flow graphs for all DISO converters. For the sake of maintaining simple nomenclature, as shown in Fig. 2, the complete power flow graph is referred to as Type I-I graph if it involves two Type I sub-graphs. Also, a Type I-II graph involves one Type I sub-graph and one Type II sub-graph, which has two variants, namely, Types I-IIA and I-IIB. Likewise, we have Type II-II power flow graph. It is worth noting that Types I-IIA and I-IIB are identical due to the spatial symmetry between inputs I and II. Since a converter is needed to transfer controlled power from an input port to an output port, two converters will be placed in appropriate paths of the power flow graphs to complete the derivation of DISO converters. For instance, for the Type II converter, there are three possible ways of placing converters. Hence, a total of thirteen configurations of DISO converters in terms of power flow graphs can be obtained, as shown in Fig. 3, where the solid square boxes denote simple converters. For simplicity, we refer to them as configurations I-I, I-IIA, I-IIB, I-IIC, II-IIA, II-IIB, II-IIC, and so on.

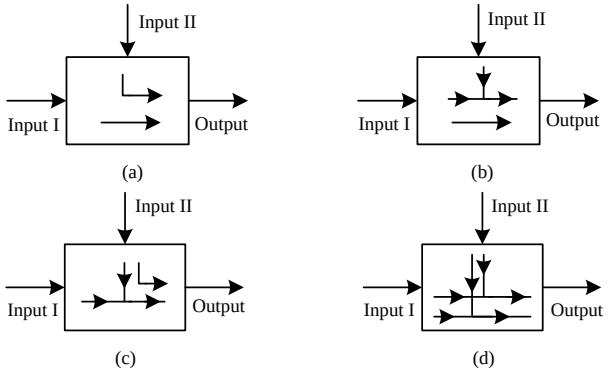

Fig. 2. Power flow graphs for DISO converters with both input ports supplying power unidirectionally. (a) Type I-I; (b) Type I-IIA; (c) Type I-IIB; (d) Type II-II.

From Fig. 3, it can be easily seen that configuration II-IIA is equivalent to configuration II-IIH, configuration II-IIB is equivalent to configuration II-IIG, and configuration II-IIC is equivalent to configuration II-IID, configuration II-IIE and configuration II-III, due to spatial symmetry. Consequently, only eight unique configurations exist for DISO converters, namely, configurations I-I, I-IIA, I-IIB, I-IIC, II-IIA, II-IIB, II-IIC, and II-IIF.

Input ports are normally defined as unidirectional entry ports where power flows into the DISO. However, if one of the input ports is connected to a battery allowing bidirectional power flow, the resulting power flow graphs will be different. For the purpose of illustration, we consider an input port being connected to a voltage source and the load is a voltage load. For the case of a DISO converter containing a battery, three types of power flow sub-graphs are relevant, as shown in Fig. 4. To avoid confusion, the ports are named input port, battery port and output port, as shown in Fig. 5. The three types of power flow sub-graphs are:

Type I: Power is transferred from one port to another port, as shown in Fig. 4(a).

Type II: Power is transferred from two ports to one port, as shown in Fig. 4(b).

Type III: Power is transferred from one port to two ports, as shown in Fig. 4(c).

Then, we can construct the complete power flow graphs for all DISO converters with a battery connected to an input port, namely Types I-I, I-II, I-III and II-III, as shown in Fig. 5. For this type of DISO converters, a converter is needed to transfer controlled power from the input port to the battery port or output port, and a bi-directional converter is required to store or transfer power from the input port to the output port. Due to spatial symmetry, only four specific configurations permit simple interconnections, namely, configurations I-IIA, I-IIB, I-IIIA and I-IIIB, as shown in Fig. 6.

III. Comparison of DISO Converters with Two Unidirectional Input Ports

From the afore-described analysis of DISO converters with both input ports supplying power unidirectionally (without battery), we see that the types of sources and loads play crucial roles in determining the control methods and the ultimate characteristics. In the following, we illustrate a case where the input ports are voltage sources and the output port provides a regulated voltage. Other cases can be studied in a likewise manner, and detailed are therefore omitted here.

A. Possible Choices

In Section II, eight (unique) possible configurations of DISO converters have been presented, each of which is composed of two basic switching converters. Each of the two basic switching converters can be either buck, boost or buck-boost converter [21], [22]. It is noteworthy that SEPIC, Cuk and Zeta converters, though are not basic converters, can also be used, provided voltage polarity and current direction are dually taken into consideration. For the purpose of maintaining a minimum configuration, we focus on the basic buck, boost and buck-boost converters here. However, not all eight configurations can be readily implemented in practical forms. Upon close inspection of these configurations, only six specific configurations permit simple interconnections, namely, configurations I-I, I-IIA, I-IIB, II-IIB, II-IIF and II-IIG (Figs. 3(a), (b), (c), (f), (j) and (k)). Since configurations II-IIB and II-IIG are spatially symmetrical due to the symmetric positions of the two input sources, the possible choices of converters 1 and 2 reduce to only five configurations, as summarized in Table I. Moreover, both converters 1 and 2 can also employ

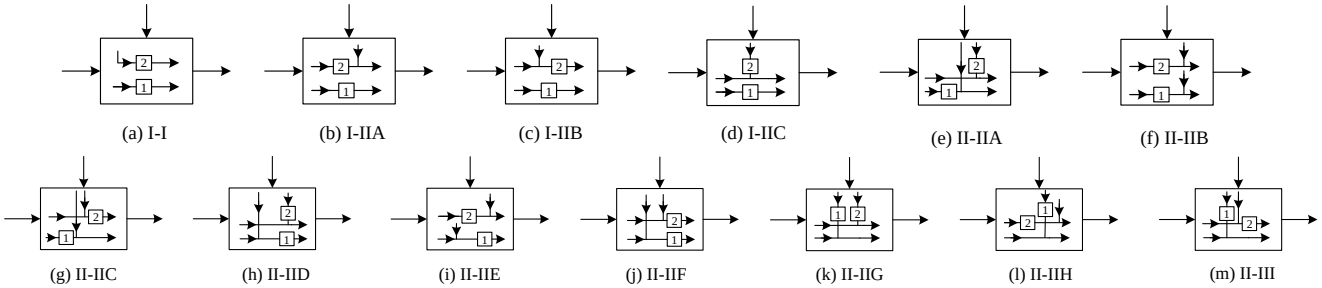

Fig. 3. Thirteen configurations of DISO converters in terms of power flow graphs

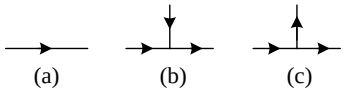

Fig. 4. Power flow sub-graphs of DISO converters with a battery connected to an input port. (a) Type I; (b) Type II; (c) Type III.

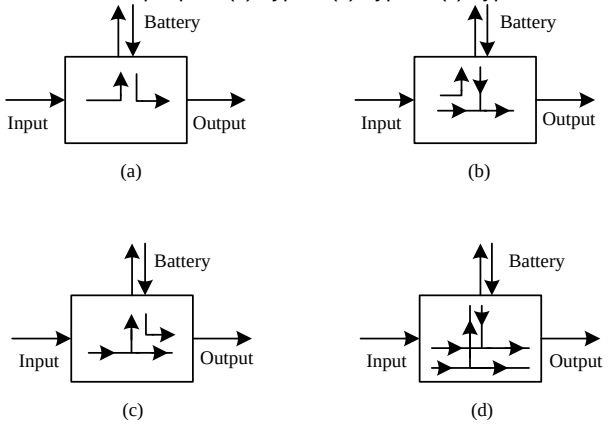

Fig. 5. Power flow graphs for DISO converters with a battery connected to an input port. (a) Type I-I; (b) Type I-II; (c) Type I-III; (d) Type II-III.

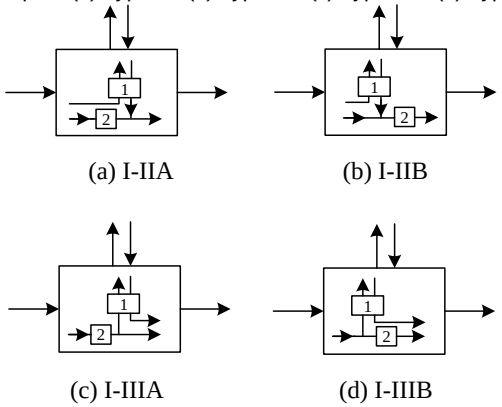

Fig. 6. Four configurations of DISO converters with a battery connected to an input port in terms of power flow graphs. (a) I-IIA; (b) I-IIB; (c) I-IIIA; (d) I-IIIB.

some transformer isolated converters or bridge-based converters to cater for high voltage and high power applications.

Now, we can construct possible DISO converters, as shown in Fig. 7. For illustration, buck converters have been used here for implementation of converters 1 and 2, corresponding to configurations I-I, I-IIA, I-IIB, II-IIB, II-IIF. Here, the isolated DISO converter can also be constructed by replacing the buck converter with the forward converter.

Realization of configuration I-I: For this configuration, converters 1 and 2 can be any converter. Suppose buck converters are used for both converters 1 and 2, as shown in Fig. 7(a). It is clear that the input sources v_{in1} and v_{in2} will transfer power to the load R independently, and both input voltage ranges of v_{in1} and v_{in2} are larger than the output voltage V_o according to Kirchhoff's voltage law (KVL).

Realization of configuration I-IIA: For this configuration, converters 1 and 2 can employ a buck or boost converter. Similar to the configuration I-I case, we employ buck converters for converters 1 and 2, as shown in Fig. 7(b) shows configuration I-IIA. Here, converters 1 and 2 share the power provided by the input source v_{in1}. The range of v_{in1} is higher than output voltage V_o, while the range of v_{in2} must be lower than output voltage V_o according to KVL.

TABLE I
POSSIBLE CHOICES OF BASIC CONVERTERS FOR DISO CONVERTERS WITH BOTH INPUT PORTS SUPPLYING POWER UNIDIRECTIONALLY

Configuration	Converter 1	Converter 2
I-I	any	any
I-IIA	Buck or Boost	Buck or Boost
I-IIB	Buck or Boost	Buck or Boost
I-IIB	Buck or Boost	Buck- Boost
II-IIB	Buck or Boost	Buck or Boost
II-IIB	Buck- Boost	Buck- Boost
II-IIF	Buck or Boost	Buck or Boost
II-IIF	Buck- Boost	Buck- Boost

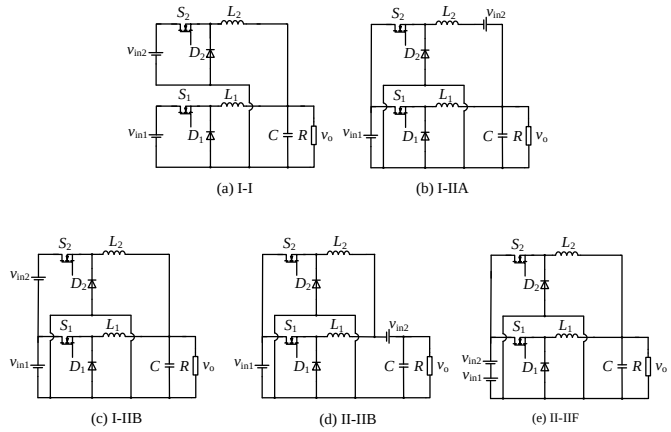

Fig. 7. Possible implementations for DISO converters with two input ports supplying power unidirectionally.

***Realization of configuration I-IIB*:** Two implementation cases are possible. In the first case, converters 1 ad 2 may employ a buck or boost converter. In the second case, converters 1 and 2 are both a buck-boost converter. Suppose converters 1 and 2 are buck converters. In a likewise manner, we obtain a new DISO converter, as shown in Fig. 7(c), where converters 1 and 2 share the power provided by the input source v_{in1}. Both input sources v_{in1} and v_{in2} provide power to converter 2. From KVL, the range of v_{in1} is higher than output voltage V_o and the range of v_{in2} is larger than zero.

***Realization of configuration II-IIB*:** The implementation possibilities of this configuration are same as configuration I-IIB. A specific example is given in Fig. 7(d), where both input sources v_{in1} and v_{in2} provide power to converters 1 and 2. Similar to the case of configuration I-IIA, the range of v_{in1} is higher than output voltage V_o, and the range of v_{in2} must be smaller than output voltage V_o.

***Realization of configuration II-IIF*:** The implementation possibilities of this configuration are same as configurations I-IIB and II-IIB. As mentioned before, we can employ buck converters for converters 1 and 2, as shown in Fig. 7(e), where input sources v_{in1} and v_{in2} are connected in series. Consequently, the sum of input sources v_{in1} and v_{in2} must be higher than output voltage V_o.

B. Control Methods

For a DISO converter with out battery, the distribution of the input power from the two sources to the output load is a key design issue, and the type of the load is considered as a crucial control specification. For voltage-type loads, a voltage loop is designed to control/regulate the output voltage, whereas for current-type loads, a current loop is set up to program the output current. Thus, the usual control objectives of a DISO converter are to regulate the output voltage or current, and to achieve a specific power flow distribution from the two input sources. The control methods of DISO converters can be developed in the light of these two objectives, as detailed in the following subsections.

For voltage loads (i.e., loads requiring regulated voltage), a voltage loop is first required to regulate the output voltage under possible fluctuations of the input sources. Then, another current loop or voltage loop is needed to achieve the required power flow distribution, the specific design being dependent upon the type of the input sources. Specifically, a current (voltage) loop is needed to control the input power from one of the input sources if it is a voltage (current) source. This is because the input power of a voltage (current) source can only be controlled by regulating the input current (voltage). Once the input power from one input source is determined, the input power from the other source is automatically defined since the total output power has already been determined by the first control loop that regulates the output voltage or current.

For current loads (i.e., loads requiring regulated current), a current loop is first required to regulate the output current. Then, another current loop or voltage loop is needed for defining the power flow distribution, depending upon the type of the input sources, as discussed above.

It should be noted that this control strategy including two independent control loops is generic. Since one simple power converter is theoretically capable of performing only one specific control function via adjusting its power flow (with duty cycle as the control variable). Thus, results based on the use of this control method are expected to be generally applicable. For specific applications requiring the use of more advanced control [23], double-loop or multiple-loop control can be designed to achieve more complex control objectives [8].

From the afore-described analysis of DISO converters, we see that the types of sources and loads play crucial roles in determining the control methods and the ultimate characteristics. In the following, we illustrate a case where the input ports are voltage sources and the output port provides a regulated voltage. Other cases can be studied in a likewise manner, and detailed are therefore omitted here.

C. Efficiency Analysis

Let η_1 and η_2 be the efficiencies of converters 1 and 2, respectively. Suppose the ratio of the input power coming from the two input sources is k :1 $-k$. Also, the input power from converter1 is split at a ratio of r to 1 $-r$ before being further processed; likewise the input power from the converter 2 is split at a ratio of f to 1 $-f$. The efficiencies of the five configurations can be obtained, as tabulated in Table II. We will show that an appropriate distribution of the power of converters 1 and 2 is crucial to optimizing the overall efficiency of the DISO converter. Also, a higher efficiency can be achieved at the expense of degraded control functions as the converters would only be partially controlled if the amount of power being processed is dictated by the efficiency optimization.

TABLE II
EFFICIENCY OF DISO CONVERTERS

Configuration	Efficiency
I-I	$k_1\eta_1+(1-k_1)\eta_2$
I-IIA	$k_2[r_1\eta_1+(1-r_1)\eta_2]+(1-k_2)\eta_2$
I-IIB	$k_3[r_2\eta_1+(1-r_2)\eta_2]+(1-k_3)\eta_2$
II-IIB	$k_4[r_3\eta_1+(1-r_3)\eta_2]+(1-k_4)[f_1\eta_1+(1-f_1)\eta_2]$
II-IIF	$k_5[r_4\eta_1+(1-r_4)\eta_2]+(1-k_5)[f_2\eta_1+(1-f_2)\eta_2]$

For configuration I-I, from Fig. 7(a), denoting the average currents of L_1 and L_2 as I_{L1} and I_{L2}, respectively, the average output current I_o equals the sum of I_{L1} and I_{L2}. Then, the ratio parameter k_1 can be obtained as

$$k_1=\frac{I_o-I_{L2}}{I_o} \tag{1}$$

For configurations I-IIA, from Fig. 7(b), denoting the average currents in switches S_1 and S_2 as I_{S1} and I_{S2}, respectively, the ratio parameters k_2 and r_1 are given by

$$k_2=\frac{V_oI_o-V_{in2}I_{L2}}{V_oI_o},\ r_1=\frac{I_{S1}}{I_{S1}+I_{S2}}=\frac{V_o(I_o-I_{L2})}{V_oI_o-V_{in2}I_{L2}} \tag{2}$$

For configuration I-IIB, from Fig. 7(c), the ratio parameters k_3 and r_2 are given by

$$k_3=1-\frac{V_{in2}I_{L2}}{I_o(V_{in1}+V_{in2})},\ r_2=\frac{(I_o-I_{L2})(V_{in1}+V_{in2})}{(V_{in1}+V_{in2})I_o-V_{in2}I_{L2}} \tag{3}$$

From (1), (2), (3) and Table II, we can see that configurations I-IIA and I-IIB have a higher efficiency than configuration I-I only if $\eta_2>\eta_1$.

For configuration II-IIB, from Fig. 7(d), the ratio parameters k_4, r_3 and f_1 are obtained as

$$k_4=\frac{V_oI_o-V_{in2}I_o}{V_oI_o},\ r_3=\frac{(V_o-V_{in2})(I_o-I_{L2})}{V_oI_o-V_{in2}I_o}=\frac{I_o-I_{L2}}{I_o}=f_1 \tag{4}$$

For configuration II-IIF, from Fig. 7(e), the ratio parameters k_5, r_4 and f_2 are given by

$$k_5=\frac{V_{in1}}{V_{in1}+V_{in2}},\ r_4=f_2=\frac{I_{S1}}{I_{S1}+I_{S2}}=\frac{I_{L1}}{I_o} \tag{5}$$

Thus, from (1), (4), (5) and Table II, if $\eta_1>\eta_2$ and $k<r$, or if $\eta_1<\eta_2$ and $k>r$, configurations II-IIB and II-IIF have a higher

efficiency than configuration I-I. Thus, the overall efficiency can be optimized by ensuring an appropriate distribution of the power of converters 1 and 2. Moreover, we should stress that efficiency and control performance are conflicting requirements, and a higher efficiency is achieved at the expense of degraded control functions, as explained previously.

D. Power Flow Distribution

As mentioned before, the power flow distribution of a DISO converter is crucial for efficiency and control optimization. For ease of description, we take the five converters presented in Fig. 7 as examples. For configuration I-I, we have

$$V_{\text{in1}}I_{\text{S1}} + V_{\text{in2}}I_{\text{S2}} = V_{\text{o}}I_{\text{o}} \tag{6}$$

In the steady state, we have

$$I_{\text{S1}} = D_{\text{ON1}}I_{\text{L1}}, \quad D_{\text{ON1}} = \frac{V_{\text{o}}}{V_{\text{in1}}} \tag{7}$$

where D_{ON1} is the duty ratio of S_1 Then, from (6) and (7), the input powers (P_1 and P_2) of converters 1 and 2 can be obtained as follows:

$$P_1 = V_{\text{in1}}I_{\text{S1}} = V_{\text{o}}(I_{\text{o}} - I_{\text{L2}}), \quad P_2 = V_{\text{in2}}I_{\text{S2}} = V_{\text{o}}I_{\text{L2}} \tag{8}$$

Likewise, we can obtain the power equations of other four configurations, as given in Table III.

TABLE III
POWER EQUATIONS OF DISO CONVERTERS

Configuration	P_1	P_2
I-I	$P_1 = V_{\text{o}}(I_{\text{o}} - I_{\text{L2}})$	$P_2 = V_{\text{o}}I_{\text{L2}}$
I-IIA	$P_1 = V_{\text{in1}}(I_{\text{S1}} + I_{\text{S2}})$	$P_2 = V_{\text{in2}}I_{\text{L2}}$
I-IIB	$P_1 = V_{\text{in1}}(I_{\text{S1}} + I_{\text{S2}})$	$P_2 = V_{\text{in2}}I_{\text{S2}}$
II-IIB	$P_1 = V_{\text{in1}}(I_{\text{S1}} + I_{\text{S2}})$	$P_2 = V_{\text{in2}}I_{\text{o}}$
II-IIF	$P_1 = V_{\text{in1}}(I_{\text{S1}} + I_{\text{S2}})$	$P_2 = V_{\text{in2}}(I_{\text{S1}} + I_{\text{S2}})$

The plots of power versus I_{L2} are shown in Fig. 8 using the following set of circuit parameters: V_{in1} = 48 V, V_{o} = 30 V, I_{o} =1 A. It is noteworthy that V_{in2} = 24Vfor configurations I-IIA and II-IIB because of the restriction of V_{in2}, and for configurations I-I, I-IIB and II-IIF, we choose V_{in2} = 36V for the simulation.

As shown in Figs. 8(a) and (b), configuration I-I has the largest input power ranges of P_1 and P_2 among the three configurations. Configuration I-IIB has smaller power range than configuration I-I (17.1-30 W and 0-12.9 W, respectively), and input powers P_1 and P_2 of configuration II-IIF are kept constant (17.1 W and 12.9W, respectively). Hence, for configuration II-IIF, the distribution of input powers P_1 and P_2 cannot be controlled because the two input ports are in series transferring power to the output port. Compared with configuration II-IIB shown in Figs. 8(c) and (d), configuration I-IIA has a larger input power range, and the distribution of input powers of P_1 and P_2 cannot be controlled for configuration II-IIB because the two input ports transfer power to the output port through both converters 1 and 2.

E. Switching Stress

Switching stresses include current stress and voltage stress. Since the current stress is different when the converter works in different operating modes, namely, continuous conduction mode (CCM) and discontinuous conduction mode (DCM), we will present the current stress of the switch in CCM and DCM.

Tables IV and V show the current stresses for CCM and DCM operation, where I_{P1} and I_{P2} are the current stresses of S_1 and S_2, respectively. The voltage stresses are summarized in Table VI, where V_{S1} and V_{S2} are the voltage stresses of S_1 and S_2, respectively.

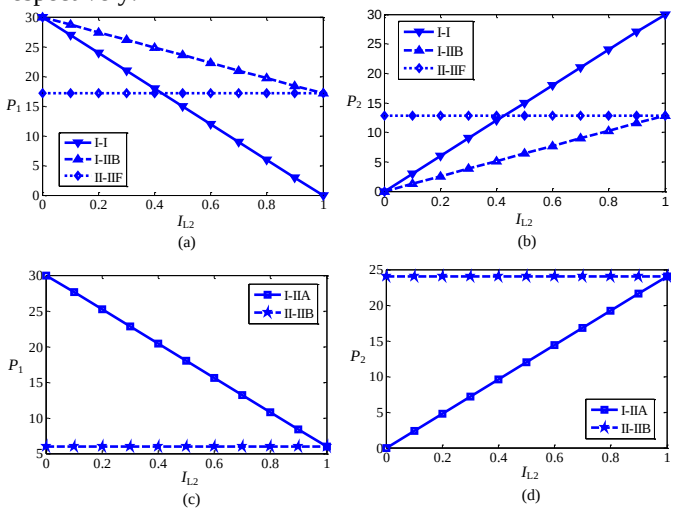

Fig. 8. Simulation results of input power versus I_{L2}. (a) P_1 of configurations I-I, I-IIB, II-IIF; (b) P_2 of configurations I-I, I-IIB, II-IIF; (c) P_1 of configurations I-IIA and II-IIB; (d) P_2 of configurations I-IIA and II-IIB.

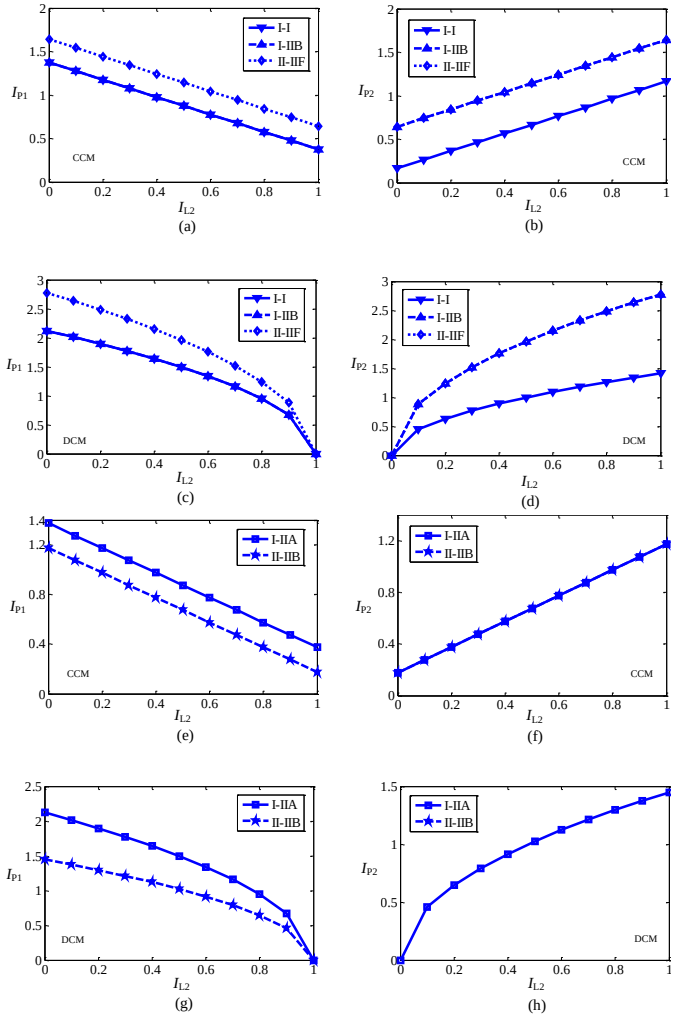

Fig. 9. Simulation results of current stresses I_{P1} and I_{P2} versus I_{L2}. (a) I_{P1} of configurations I-I, I-IIB and II-IIF in CCM; (b) I_{P2} of configurations I-I,

TABLE IV
CURRENT STRESS OF S_1 AND S_2 IN CCM

Configuration	Current stress	
	Converter1	Converter2
I-I	$I_{P1}=\frac{2V_{in1}L_1I_{L1}+V_o(V_{in1}-V_o)T}{2V_{in1}L_1}$	$I_{P2}=\frac{2V_{in2}L_2I_{L2}+V_o(V_{in2}-V_o)T}{2V_{in2}L_2}$
I-IIA	$I_{P1}=\frac{2V_{in1}L_1I_{L1}+V_o(V_{in1}-V_o)T}{2V_{in1}L_1}$	$I_{P2}=\frac{2V_{in1}L_2I_{L2}+(V_o-V_{in2})(V_{in1}+V_{in2}-V_o)T}{2V_{in1}L_2}$
I-IIB	$I_{P1}=\frac{2V_{in1}L_1I_{L1}+V_o(V_{in1}-V_o)T}{2V_{in1}L_1}$	$I_{P2}=\frac{2(V_{in1}+V_{in2})L_2I_{L2}+V_o(V_{in1}+V_{in2}-V_o)T}{2(V_{in1}+V_{in2})L_2}$
II-IIB	$I_{P1}=\frac{2V_{in1}L_1I_{L1}+(V_o-V_{in2})(V_{in1}+V_{in2}-V_o)T}{2V_{in1}L_1}$	$I_{P2}=\frac{2V_{in1}L_2I_{L2}+(V_o-V_{in2})(V_{in1}+V_{in2}-V_o)T}{2V_{in1}L_2}$
II-IIF	$I_{P1}=\frac{2(V_{in1}+V_{in2})L_1I_{L1}+V_o(V_{in1}+V_{in2}-V_o)T}{2(V_{in1}+V_{in2})L_1}$	$I_{P2}=\frac{2(V_{in1}+V_{in2})L_2I_{L2}+V_o(V_{in1}+V_{in2}-V_o)T}{2(V_{in1}+V_{in2})L_2}$

TABLE V
CURRENT STRESS OF S_1 AND S_2 IN DCM

Configuration	Current stress	
	Converter1	Converter2
I-I	$I_{P1}=\sqrt{\frac{2(V_{in1}-V_o)V_oTI_{L1}}{V_{in1}L_1}}$	$I_{P2}=\sqrt{\frac{2(V_{in2}-V_o)V_oTI_{L2}}{V_{in2}L_2}}$
I-IIA	$I_{P1}=\sqrt{\frac{2(V_{in1}-V_o)V_oTI_{L1}}{V_{in1}L_1}}$	$I_{P2}=\sqrt{\frac{2(V_{in1}+V_{in2}-V_o)(V_o-V_{in2})TI_{L2}}{V_{in1}L_2}}$
I-IIB	$I_{P1}=\sqrt{\frac{2(V_{in1}-V_o)V_oTI_{L1}}{V_{in1}L_1}}$	$I_{P2}=\sqrt{\frac{2(V_{in1}+V_{in2}-V_o)V_oTI_{L2}}{(V_{in1}+V_{in2})L_2}}$
II-IIB	$I_{P1}=\sqrt{\frac{2(V_{in1}+V_{in2}-V_o)(V_o-V_{in2})TI_{L1}}{V_{in1}L_1}}$	$I_{P2}=\sqrt{\frac{2(V_{in1}+V_{in2}-V_o)(V_o-V_{in2})TI_{L2}}{V_{in1}L_2}}$
II-IIF	$I_{P1}=\sqrt{\frac{2(V_{in1}+V_{in2}-V_o)V_oTI_{L1}}{(V_{in1}+V_{in2})L_1}}$	$I_{P2}=\sqrt{\frac{2(V_{in1}+V_{in2}-V_o)V_oTI_{L2}}{(V_{in1}+V_{in2})L_2}}$

I-IIB and II-IIF in CCM; (c) I_{P1} of Configurations I-I, I-IIB and II-IIF in DCM; (d) I_{P2} of configurations I-I, I-IIB and II-IIF in DCM; (e) I_{P1} of configurations I-IIA and II-IIB in CCM; (f) I_{P2} of configurations I-IIA and II-IIB in CCM; (g) I_{P1} of configurations I-IIA and II-IIB in DCM; (h) I_{P2} of configurations I-IIA and II-IIB in DCM.

Current stresses of a DISO converter operating in CCM and DCM can be found for given sets of circuit parameters: (1) V_{in1} = 48V, V_{in2} = 36V, V_o = 30V, I_o =1A, T = 20 μs, $L_1 = L_2$ = 300 μH for CCM, $L_1 = L_2$ = 100 μH for DCM; (2) V_{in1} = 48V, V_{in2} = 24V, V_o = 30 V, I_o =1A, T = 20 μs, $L_1 = L_2$ = 300 μH for CCM, $L_1 = L_2$ = 100 μH for DCM.

Parameter set (1) is used for configurations I-I, I-IIB and II-IIF, and parameter set (2) is used for configurations I-IIA and II-IIB. Fig. 9 shows the current stresses of S_1 and S_2 of DISO converters operating in CCM and DCM.

From Figs. 9(a), (b), (c), (d) and Table VI, comparing with configurations I-IIB and II-IIF, configuration I-I has the lowest current stress for both DCM and CCM, as well as the lowest voltage stress. Compared with configuration I-IIA, configuration II-IIB has lower current stress in S_1 for both DCM and CCM.

F. Note on Applications

From the foregoing simulation and analytical results, we may summarize the general application areas of the five configurations. In short, configurations I-I, I-IIA and I-IIB can be used in applications where multiple input sources or wide ranges of input power are needed, such as in hybrid systems of distributed generation and delivery via power grid [24]-[26]. Furthermore, configuration I-I has the highest power efficiency if the difference in efficiencies in the two converters is properly exploited, and it also has the lowest switching stress among the three configurations. Thus, configuration I-I is the optimal choice in application areas where wide ranges of input power, high efficiency or low switching stress are needed. Also, since configurations II-IIB and II-IIF have constant input power, they can be used for applications where control of power distribution is less critical such as in interleaved paralleled converters for reducing the input current ripple [27].

TABLE VI
VOLTAGE STRESS OF S_1 AND S_2

Configuration	Current stress	
	Converter1	Converter2
I-I	$V_{S1}=V_{in1}$	$V_{S2}=V_{in2}$
I-IIA	$V_{S1}=V_{in1}$	$V_{S2}=V_{in1}$
I-IIB	$V_{S1}=V_{in1}$	$V_{S2}=V_{in1}+V_{in2}$
II-IIB	$V_{S1}=V_{in1}$	$V_{S2}=V_{in1}$
II-IIF	$V_{S1}=V_{in1}+V_{in2}$	$V_{S2}=V_{in1}+V_{in2}$

IV. COMPARISON OF DISO CONVERTERS WITH ONE INPUT PORT CONNECTED TO A BATTERY

A. Possible Choices

In Fig. 6, four possible configurations of DISO converters with a battery connected to an input port are presented. Each configuration is composed of two basic switching converters. Converter 1 can be either buck or boost converter, and converter 2 should be a bidirectional converter. Due to the bidirectional characteristic of converter 2, configurations I-IIA and I-IIIB are equivalent. Hence, only three configurations

exist for DISO converters with a battery connected to an input port. The possible choices of converters 1 and 2 are summarized in Table VII. Moreover, both converters 1 and 2 can also employ some transformer isolated converters or bridge-based converters to cater for high voltage and high power applications. Then, we can also construct DISO converters with a battery connected to an input port, as shown in Fig. 10. For illustration, the buck converter has been used here for implementation of converter 1, and a bidirectional buck-boost converter has been used for implementation of converter 2.

B. Control Methods

From Fig. 5, we can see that input port is the main power source, and the battery serves as the back up power source. Hence, for this DISO converter, there are two key design issues. First, the output port is needed to supply regulated voltage or current. Second, the battery should be charged or discharged appropriately. A voltage loop is first required to regulate the output voltage under possible fluctuations of the input sources. Then, according to the input power and output power, the bidirectional converter is used to charge the battery or to power the load. If the battery is supplying power to the load, the control method is the same as described in the previous section. However, if the battery is drawing power (being charged), constant output current is designed when the battery is not in full state, and constant output voltage is designed when the battery is fully charged. It is worth noting that if the input port is connected to a solar power source, maximum power point tracking (MPPT) should be incorporated in the control system.

TABLE VII
POSSIBLE CHOICES OF BASIC CONVERTERS FOR DISO CONVERTERS WITH A BATTERY CONNECTED TO AN INPUT PORT

Configuration	Converter 1	Converter 2
I-IIA	Buck or Boost	Bidirectional Buck-Boost Converter
I-IIB	Buck or Boost	Bidirectional Buck-Boost Converter
I-IIIA	Buck or Boost	Bidirectional Buck-Boost Converter

C. Efficiency Analysis

From Fig. 6, there are three power transmission loops. First, the input port transfers power to the output port. Second, the battery port stores (draws) power from the input port. Third, the battery port discharges power to the output port. For configuration I-IIB, both converters 1 and 2 (two converter stages) are needed to discharge power from the battery port to the output port. For configuration I-IIIA, both converters 1 and 2 (two converter stages) are also needed to transfer power from the input port to the battery port. However, for configurations I-IIA, only one converter (converter 1 or converter 2) is needed to transfer or store power among the three ports. As discussed previously, it is easy to see that the efficiency of configuration I-IIA is higher than that of configurations I-IIB and I-IIIA. Efficiency analysis can be further discussed as follows.

Let η_3 and η_4 be the efficiency of converters 1 and 2, respectively. Suppose the ratio of the input power splitting to the battery and to the load is α: 1-α. Also, the ratio of the input power coming from the input port and the battery is β: 1-β. Likewise, the ratio of the charging time to the discharging time for the battery is γ: 1-γ. The efficiencies of the three configurations can be obtained, as tabulated in Table VIII.

TABLE VIII
EFFICIENCY OF DISO CONVERTERS WITH A BATTERY CONNECTED TO AN INPUT PORT

Configuration	Efficiency
I-IIA	$\gamma[\alpha\eta_3+(1-\alpha)\eta_4]+(1-\gamma)[\beta\eta_3+(1-\beta)\eta_4]$
I-IIB	$\gamma[\alpha\eta_3+(1-\alpha)\eta_4]+(1-\gamma)[\beta\eta_3+(1-\beta)\eta_3\eta_4]$
I-IIIA	$\gamma[\alpha\eta_3+(1-\alpha)\eta_3\eta_4]+(1-\gamma)[\beta\eta_3+(1-\beta)\eta_4]$

From Table VIII, the difference in the efficiency between configurations I-IIA and I-IIB can be obtained as

$$\Delta P_1 = (1-\gamma)(1-\beta)(1-\eta_3)\eta_4 \tag{9}$$

and the difference in efficiency between configurations I-IIA and I-IIIA is obtained as

$$\Delta P_2 = \gamma(1-\alpha)(1-\eta_3)\eta_4 \tag{10}$$

From (9) and (10), we can see that configuration I-IIA has the highest efficiency than configurations I-IIB and I-IIIA, and the larger the value of β and γ, the closer the efficiency between configurations I-IIA and I-IIB. This means the efficiency of configuration I-IIB is expected be much higher with less discharging time and discharging energy. Moreover, the larger the value of α or the smaller the value of γ, the closer the efficiency between configurations I-IIA and I-IIIA. Thus, we see that the efficiency of configuration I-IIIA becomes much higher with less charging time and charging energy.

From the foregoing analytical results, we may conclude that configuration I-IIA is the optimal choice in application areas where high efficiency is needed, such as in hybrid distributed power systems [28], [29].

V. EXPERIMENTAL VERIFICATION

To verify the analysis and simulation results given above, experimental measurements of a DISO converter with both input ports supplying power unidirectionally are performed with the same circuit parameters as listed in Section III. We choose the circuit of Fig. 7(a) for the purpose of illustration. Fig.

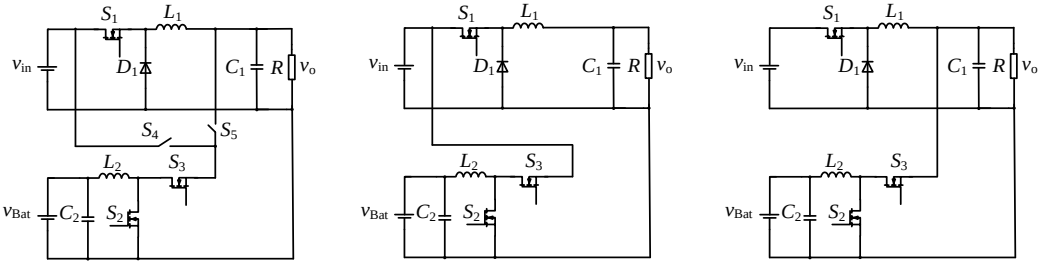

(a) I-IIA (b) I-IIB (c) I-IIIA

Fig. 10. Possible implementations for DISO converters with a battery connected to an input port

11 shows the schematic of the circuit. The control loops consist of a voltage loop which uses a amplifier LT1357 and a comparator LM319 for regulating the output voltage, and a current loop that employs two amplifiers LT1357 and a comparator LM319 for distributing the output power. Also, the output of amplifier LT1357 and sawtooth voltage V_{saw} are applied at the input of the comparator LM319 to generate control pulses for switches S_1 and S_2. It is should be noted that the two sawtooth voltages V_{saw} of the voltage and current loops are provided from the same source to keep the synchronization of the control pulses. Furthermore, IR2125 is the driver IC.

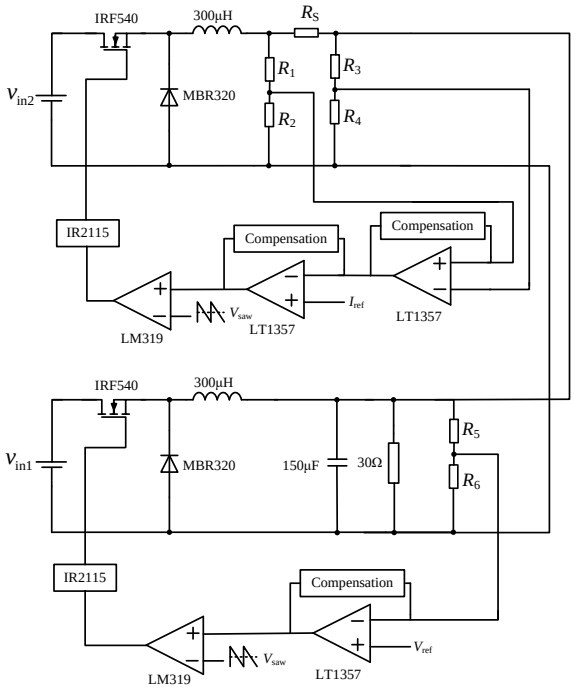

Fig. 11. Schematic of experimental DISO converter [Fig. 7(a)]

Fig. 12 shows the waveforms of inductor current, output voltage and sawtooth voltage V_{saw} with the reference currents set at 0.5 A and 0.3 A. From Fig. 12, we see that the inductor currents are effectively regulated to achieve the required power distribution, and the output voltage is stable.

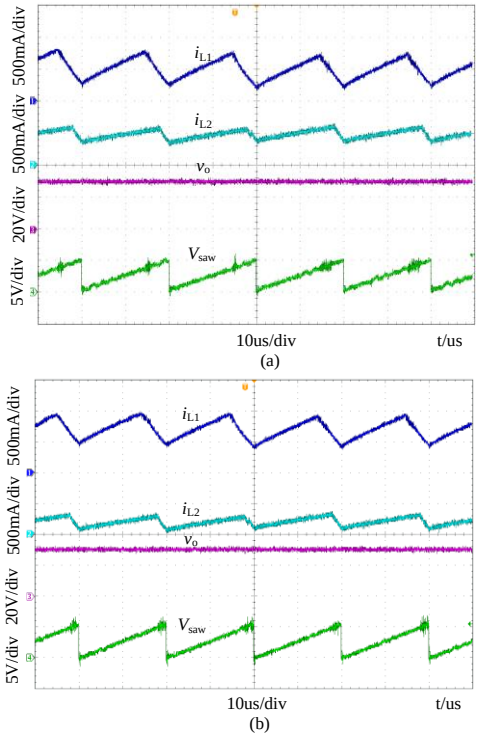

Fig. 12. Experimental results of DISO converter. (a) I_{L2} is 0.5A; (b) I_{L2} is 0.3A

Fig. 13(a) shows the variation of k against I_{L2}. Here, we see that k decreases with the increase of I_{L2} for configurations I-I, I-IIA and I-IIB, and k is kept constant for configurations II-IIB and II-IIF. Figs. 13(b) to (f) compare the efficiency of the

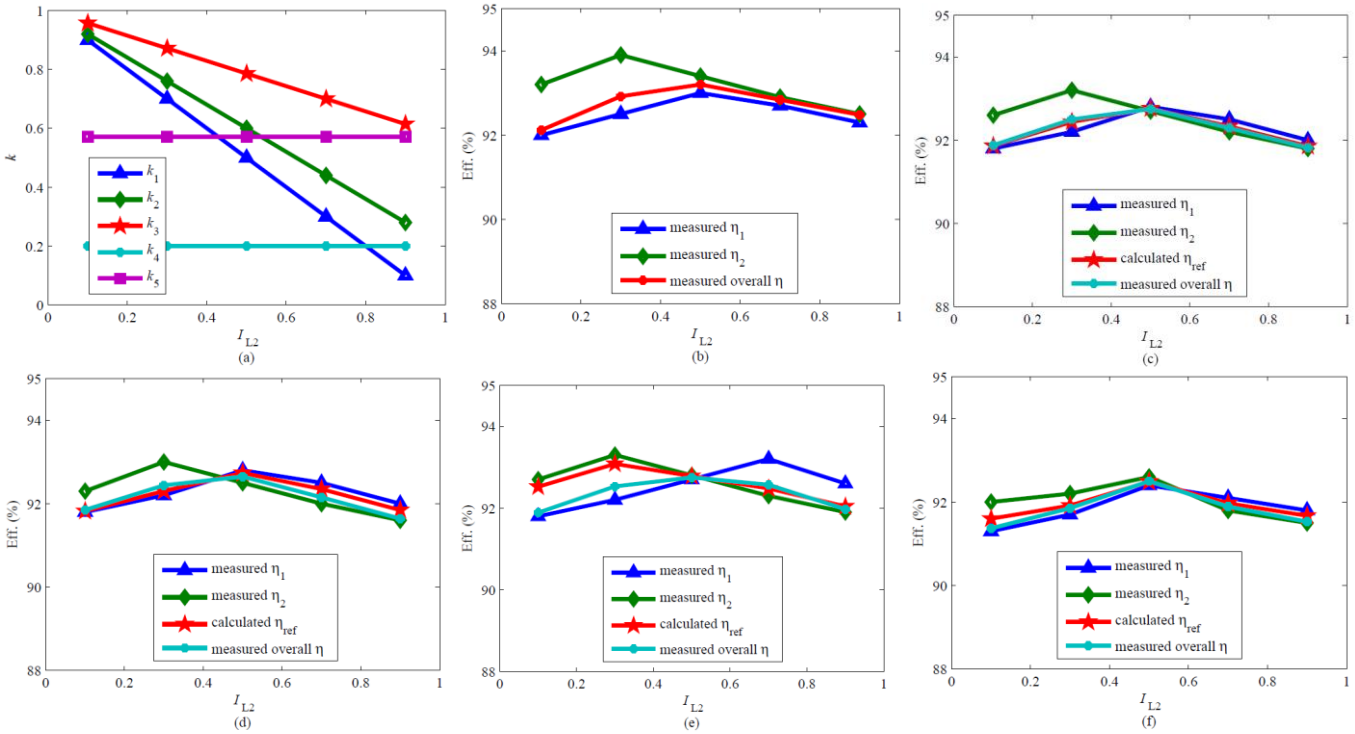

Fig. 13. Possible implementations for DISO converters with a battery connected to an input port

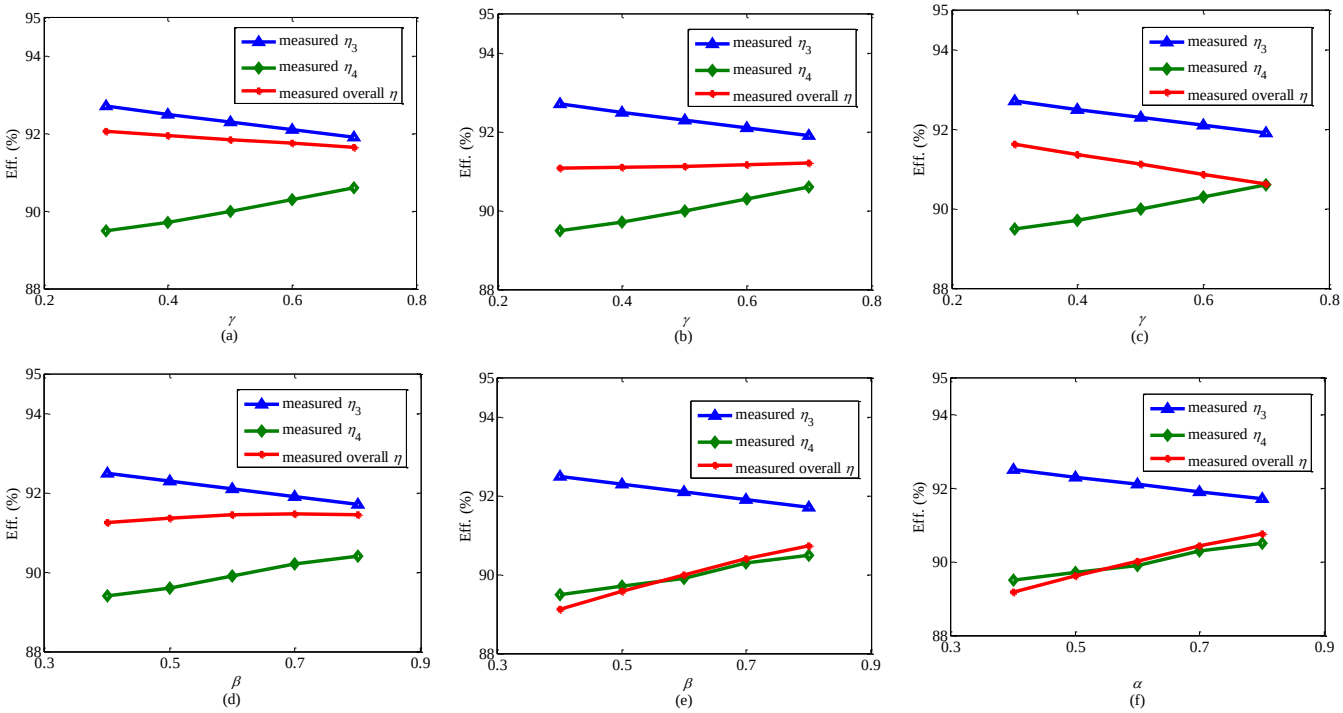

Fig. 14. Experimental results of efficiencies versus ratio of charging time to discharging time γ for (a) configuration I-IIA; (b) configuration I-IIB; (c) configuration I-IIIA; efficiencies versus ratio of power from input port and from battery port β for (d) configuration I-IIA; (e) configuration I-IIB; efficiencies versus ratio of power split to battery port and to load α for (f) configuration I-IIIA

various configurations versus I_{L2}, with I_{L2} varying from 0 to 1 A, where η_{ref} in Figs. 13(c) to (f) is the efficiency of configuration I-I shown earlier in Table II.

From Fig. 13(b), we can see that when I_{L2} increases (i.e., k decreases), the efficiency is determined by the relationship between η_1 and η_2. Thus, if η_1 and η_2 are higher, the overall efficiency is higher, and vice versa. When I_{L2} is 0.5 A, the efficiency reaches a maximum because of the maximum weighted average of η_1 and η_2. From Figs. 13(c) and (d), we observe that only if $\eta_2 > \eta_1$, the overall efficiency is higher than η_{ref}. Also, from Fig. 13(e), we see that the overall efficiency is higher than η_{ref} only if $\eta_2 < \eta_1$ and I_{L2} increases to 0.7 A (i.e., $k < r$). Also, from Fig. 13(f), we see that when $\eta_2 > \eta_1$ and I_{L2} increases to 0.5 A (i.e., $k > r$), the overall efficiency is higher than η_{ref}. In conclusion, the efficiency analysis results agree with the analytical results presented in Section III.

For the DISO converter with a battery connected to an input port, we illustrate a case where converter 1 is a buck converter and converter 2 is a bidirectional buck-boost converter using the following set of circuit parameters: V_{in} = 150 V, V_{Bat} = 48 V, V_o = 100 V, I_o = 2A.

Figs. 14(a) to (c) show the variation of γ against the efficiencies of the three configurations. Here, we see that configuration I-IIA has a higher efficiency than configurations I-IIB and I-IIIA. Figs. 14 (d) to (f) compare the efficiencies of the various configurations versus β and α. Here, it can be seen that when β increases, the efficiency of configuration I-IIB is close to that of configuration I-IIA, and when α increases, the efficiency of configuration I-IIIA is close to that of configuration I-IIA. In conclusion, the efficiency analysis results are consistent with the analytical results presented in Section IV.

VI. Conclusion

A systematic procedure based on power flow graphs has been derived for generating double-input single-output converters. Control methods are discussed, considering that the two input ports can be connected to a voltage source or current source and the output port can be connected to a load requiring regulated voltage or current. Taking the DISO converter with two voltage sources and one voltage load as an example, efficiency analysis, power distribution, and switching stress are discussed. We have demonstrated that power distribution and efficiency can be optimized for specific applications. In particular, the overall efficiency of DISO converter can be improved by controlling the power flow distribution. In practice, by biasing a higher power flow to an efficient converter, the overall efficiency of a DISO converter can be enhanced. In addition, for the special case a battery that exists in DISO converter, possible for converter, control method and efficiency are also been investigated, the analysis results shows configurations I-IIA is a optimal choice in application areas where high efficiency are needed, such as in hybrid distributed power systems. Our study here provides a comprehensive guideline for synthesizing circuits and designing the power stages to achieve optimized overall efficiency.

References

[1] Y. M. Chen, Y. C. Liu, S. C. Hung, and C. S. Cheng, "Multi-input inverter for grid-connectedhybrid PV/wind power system," *IEEETrans. Power Electron.*, vol. 22, no. 3, pp. 1070–1077, May 2007.

[2] Q. Mei, X. Zhen-lin, and W.Wu, "A novel multi-port DC-DC converter for hybrid renewable energy distributed generation systems connected to power grid," in *Proc. IEEE ICIT*, Chengdu, China, Apr. 2008, pp. 1–5.

[3] K. Kobayashi, H. Matsuo, and Y. Sekine, "Novel solar-cellpower supply system using a multiple-input DC-DC converter," *IEEE Trans. Ind. Electron.*, vol. 53, no. 1, pp. 281–286, Feb. 2006.
[4] X. Zhu, X. Li, G. Shen and D. Xu, "Design of the dynamic power compensation for PEMFC distributed power system," *IEEETrans. Ind. Electron.*, vol. 57, no. 6, pp. 1935–1944, June 2010.
[5] H. J. Chiu, C. J.Yao, and Y. K. Lo, "A DC-DC converter topology for renewable energy systems," *Int.J. Circ. Theor. Appl.*, vol. 37, no. 3, pp. 485–495, July 2009.
[6] D.Yang, M.Yang, and X. Ruan, "One-cycle control fora double-input DC-DC converter," *IEEE Trans. Power Electron.*, vol. 27, no. 11, pp. 4646–4655, Nov. 2012.
[7] R. Ahmadi, H. Zargarzadeh, and M. Ferdowsi, "Nonlinear power sharing controller for a double-input hbridge-based buckboost-buckboost con-verter," *IEEE Trans. Power Electron.*, vol. 28, no. 5, pp. 2402–2414, May 2013.
[8] Y. M. Chen, Y. C. Liu, and S. H. Lin, "Double-input PWM DC-DC converter for high/low voltage sources," *IEEETrans. Ind. Electron.*, vol. 53, no. 5, pp. 1538–1544, Oct. 2006.
[9] H. Wu, K. Sun, S. Ding, and Y. Xing, "Topology derivation of noniso-lated three-port DC-DC converters from DIC and DOC," *IEEE Trans. Power Electron.*, vol. 28, no. 7, pp. 3297–3307, July 2013.
[10] F. Liu, Z. Wang, Y. Mao, and X. Ruan, "Asymmetrical half-bridge double-input DC-DC converters adopting pulsating voltage source cells for low power applications," *IEEETrans.Power Electron.*, vol. 29, no. 9, pp. 4741–4751, Sep. 2014.
[11] Y. Li, X. Ruan, D.Yang,F. Liu, and C. K. Tse, "Synthesis of multiple-input DC-DC converters," *IEEETrans.Power Electron.*, vol. 25, no. 9, pp. 2372–2385, Sep. 2010.
[12] H. Matsuo, W. Lin, F. Kurokawa, T. Shigemizu, and N. Watanabe, "Characteristic of the multiple-input DC-DC converter," *IEEE Trans. Ind. Electron.*, vol. 51, no. 3, pp. 625–631, June 2004.
[13] B. G. Dobbs and P. L. Chapman, "A multiple-input DC-DC converter topology," *IEEEPower Electron. Lett.*, vol. 1, no. 1, pp. 6–9, Mar. 2003.
[14] A. Kwasinski, "Identifiation of feasible topologies for multiple-input DC-DC converters," *IEEE Trans. Power Electron.*, vol. 24, no. 3, pp. 856–861, Mar. 2009.
[15] Y. C. Liu and Y. M. Chen, "A systematic approach to synthesizing multiple-input DC-DC converter," *IEEE Trans. Power Electron.*, vol. 24, no. 1, pp. 116–127, Jan. 2009.
[16] K. Jin,X. Ruan, M.Yang and M. Xu, "A hybrid fuel cell power system," *IEEETrans. Ind. Electron.*, vol. 56, no. 4, pp. 1212–1222, April 2009.
[17] T. Hirose and H. Matsuo, "Standalone hybrid wind-solar power gener-ation system applying dump power control without dump load," *IEEE Trans. Ind. Electron.*, vol. 59, no. 2, pp. 988–997, Feb. 2012.
[18] S. Kim, J. Jeon, C. Cho, J. Ahn, and S. Kwon, "Dynamic modeling and controlofa grid-connectedhybrid generation system withversatile power transfer," *IEEE Trans. Ind. Electron.*, vol. 55, no. 4, pp. 1677– 1688, April 2008.
[19] C. K. Tse, M. H. L. Chow, and M. K. H. Cheung, "A family of PFC voltage regulator confiurations with reduced redundant power processing," *IEEE Trans. Power Electron.*, vol. 16, no. 6, pp. 794–802, Nov. 2001.
[20] C. K. Tse, "Circuit theory of power factor correctionin switching power converters," *Int.J. Circ. Theor. Appl.*, vol. 31, no. 2, pp. 157–198, Mar. 2003.
[21] G. Zhou and J. Xu, "Digital peak current control for switching DC-DC converters with asymmetrical dual-edge modulation," *IEEE Trans. Circ. Syst. II: Exp. Briefs*, vol. 56, no. 11, pp. 815–819, Nov. 2009.
[22] Y. Huang and C. K. Tse, "Circuit theoretic classifiation of parallel connected DC-DC converters," *IEEE Trans. Circ. Syst. I: Reg. Papers*, vol. 54, no. 5, pp. 1099–1108, May 2007.
[23] X. Xiong, C. K. Tse, and X. Ruan, "Bifurcation analysis of standalone photovoltaic-battery hybrid power system," *IEEE Trans. Circ. Syst. I: Reg.Papers*, vol. 60, no. 5, pp. 1354–1365, May 2013.
[24] O. Hegazy, J. V. Mierlo, and P. Lataire, "Analysis, modeling, and implementation of a multidevice interleaved DC-DC converter for fuel cell hybrid electricvehicles," *IEEE Trans.Power Electron.*, vol. 27, no. 11, pp. 4445–4458, Nov. 2012.
[25] E. Jamshidpour, B. Nahid-Mobarakeh, P. Poure, S. Pierfederici, F. Meibody-Tabar, and S. Saadate, "Distributed active resonance sup-pressionin hybrid DC power systems under unbalanced load conditions," *IEEE Trans. Power Electron.*, vol. 28, no. 4, pp. 1833–1842, Apr. 2013.
[26] G. Carli and S. S. Williamson, "Technical considerations on power con-version for electric and plug-in hybrid electric vehicle battery charging in photovoltaic installations," *IEEE Trans. Power Electron.*, vol. 28, no. 12, pp. 5784–5792, Dec. 2013.
[27] Y. Gu and D. Zhang, "Interleaved boost converter with ripple cancella-tion network," *IEEE Trans. Power Electron.*, vol. 28, no. 8, pp. 3860– 3869, Aug. 2013.
[28] S. N. Motapon, L. A. Dessaint, K. Al Haddad, "A Comparative study of energy management schemes for a fuel cell hybrid emergency power system of more electric aircraft," *IEEE Trans. Ind. Electron.*, vol. 61, no. 3, pp. 1320-1334 , March 2014.
[29] S. N. Motapon, L. A. Dessaint, K. Al Haddad, "A Robust H_2-Consumption-Minimization-Based energy management strategy for a fuel cell hybrid emergency power system of more electric Aircraft," *IEEE Trans. Ind. Electron.*, vol. 61, no. 11, pp. 6148-6156 , Nov. 2014.

Ping Yang received the B.S. degree in electrical engineering and automation, M.S. degree in mechanical and electronic engineering from Guilin University of Electronic and Technology, Guilin, China, in 2006 and 2009, respectively, and Ph.D. degree in electrical engineering from Southwest Jiaotong University, Chengdu, China, in 2013. Since December 2014, she has been a lecturer of electronic engineering at Southwest Jiaotong University. From February to June 2011, she was a Research Assistant with the Department of Electronic and Information Engineering, Hong Kong Polytechnic University, Kowloon, Hong Kong, and from September 2013 to October 2014, she was a Research Associate at the same department. Her current research interests include modulation and control techniques of power electronics systems, dynamical modeling and analysis of switching power converters.

Chi K. Tse (M'90--SM'97--F'06) received the BEng (Hons) degree with first class honors and the PhD degree from the University of Melbourne, Australia, in 1987 and 1991, respectively. He is presently Chair Professor of Electronic Engineering at the Hong Kong Polytechnic University, Hong Kong. His research interests include complex network applications and power electronics.

Jianping Xu (M'10) received the B.S. and Ph.D. degrees in electronic engineering from the University of Electronics Science and Technology of China, Chengdu, Sichuan, China, in 1984 and 1989, respectively.Since 1989, he has been with the School of Electrical Engineering, Southwest Jiaotong University, Chengdu 610031, China, where he has been a Professor since 1995. From November 1991 to February 1993, he was with the Department of Electrical Engineering, University of Federal Defense Munich, Germany, as a Visiting Research Fellow. From February 1993 to July 1994, he was with the Department of Electrical Engineering and Computer Science, University of Illinois at Chicago, as a Visiting Scholar. His research interests include modeling, analysis, and control of power electronic systems.

Guohua Zhou (S'10-M'12-SM'14) received the B.S. degree in electronic and information engineering, the M.S. and Ph.D. degrees in electrical engineering from Southwest Jiaotong University, Chengdu, China, in 2005, 2008 and 2011, respectively, where he is currently an Associate Professor in the School of Electrical Engineering.From Mar. 2010 to Sept. 2010, he was a Research Assistant with the Department of Electronic and Information Engineering, Hong Kong Polytechnic University, Kowloon, Hong Kong. From Oct. 2010 to Mar. 2011, he was a Visiting Scholar (also a Joint Ph.D. student) with

the Center for Power Electronics Systems, Virginia Polytechnic Institute and State University, Blacksburg, USA. His current research interests include modulation and control techniques of power electronics systems, dynamical modeling and analysis of switching power converters, and renewable energy applications of power electronics.